Analysis of Magnetic Properties of Soft Magnetic Composite Using Discrete Element Method

Akito Maruo[1], Hajime Igarashi[1], *IEEE Member*

[1] Graduate School of Information Science and Technology, Hokkaido University, Sapporo 060-0814, Japan

Soft Magnetic Composite (SMC), which consists of insulated iron particles, has been used for electric machines and devices. The magnetic permeability of SMC is underestimated when it is assumed that SMC is composed of homogeneous particles without magnetic contact. In this work, SMC is modeled by the discrete element method considering inhomogeneity in particle size and contact among particles. It is shown that the measured permeability of SMC can be reproduced by considering these effects. Moreover, the frequency characteristics of SMC is evaluated by the proposed method, and Ollendorff formula modified with an anomaly factor is introduced.

***Index Terms*— Anomaly Factor, Discrete Element Method, Magnetic Permeability, Ollendorff formula, Soft Magnetic Composite.**

I. Introduction

SOFT MAGNETIC COMPOSITE (SMC), which is composed of insulated iron particles, has widely been used for electric machines and devices. Because of its fine structure, SMC has advantages in high frequency applications. For the numerical analysis of the magnetic permeability and iron loss, it has been assumed that SMC is made of insulated iron particles of the same size [1-2]. The permeability has also been evaluated by the Ollendorff formula [3], which implicitly assumes the homogeneous particles without contact. It has been pointed out that the permeability of SMC is underestimated when neglecting the particle inhomogeneity and those contact [4]. Although the magnetic circuit method can take the magnetic contact among the particles into account [5], it is still difficult to consider the inhomogeneity in the particle size that makes the magnetic circuit complicated.

In this paper, we propose to use Discrete Element Method (DEM) [6] to consider both particle inhomogeneity and magnetic contact. In this method, the iron particles with different radii are generated and the motion of those particles is dynamically analyzed considering mutual mechanical contacts to simulate the formation of SMC. The magnetic permeability of the simulated SMC is computed using finite element method (FEM). We will discuss the effect of the inhomogeneity in the particle size and the magnetic contact on the magnetic permeability of SMC using the proposed method. Moreover, the frequency dependence of the magnetic permeability of SMC will also be analyzed using the proposed method.

II. Modeling method

A. *Discrete Element Method*

DEM allows us to analyze the dynamical motion of particles considering the mechanical interactions among them [6]. The equations of motion given by

$$m_i \ddot{\boldsymbol{u}}_i = \sum_j \boldsymbol{f}_{ij} + m_i \boldsymbol{g} \tag{1}$$

$$I_i \ddot{\boldsymbol{\phi}}_i = \sum_j \boldsymbol{T}_{ij} \tag{2}$$

are here solved by DEM for dynamical analysis of particles in a gravitational field, where $m, \boldsymbol{u}, \boldsymbol{g}, I$ and $\boldsymbol{\phi}$ are mass, displacement, gravitational acceleration, moment of inertia and rotational displacement, respectively. Moreover, $\boldsymbol{f}_{ij}$ and $\boldsymbol{T}_{ij}$ are interaction force and rotational moment due to mechanical contact between the *i*- and *j*-th particles.

The following procedures are executed in our DEM code:

(i) Particles with different radii are placed randomly.

(ii) Collisions are detected from the following condition

$$r_i + r_j \geq d_{i,j}, \qquad d_{i,j} = \left\| \boldsymbol{x}_i - \boldsymbol{x}_j \right\|_2 \tag{3}$$

where r, x denote the particle radius and position vector, respectively.

(iii) The interaction force among particles is computed.

(iv) Particle motion is analyzed by solving (1) and (2).

(v) Return to step (ii) if the number of steps is less than the given number. Otherwise, procedure is stopped.

B. *Modeling of SMC*

In this work, we assume that the system is two-dimensional for simplicity. The three-dimensional extension would not be difficult. We generate particles whose radii obey the Gaussian distribution, average 5μm [4], standard deviation 1.2μm, in the domain, 100 × 200μm. The values of the physical parameters are summarized in Table I. The parameters are tuned so that the system converges to the final state within practical computing time because we have interest not in the transient but in the final state. At the initial stage of simulation, particles are generated randomly so that they do not overlap each other in the domain as shown in Fig. 1 (a). Then, the particles and a thin wall with a mass start free-falling. They fall into the final positions after sufficiently long time as shown in Fig. 1 (b). The domain Ω below the wall obtained at the final state is regarded as a model of SMC. Because the final state depends on the initial condition, four additional trials are performed to have the results shown in

Manuscript received April 1, 2015; revised May 15, 2015 and June 1, 2015; accepted July 1, 2015. Date of publication July 10, 2015; date of current version July 31, 2015. (Dates will be inserted by IEEE; “published” is the date the accepted preprint is posted on IEEE Xplore®; “current version” is the date the typeset version is posted on Xplore®). Corresponding author: A. Maruo (e-mail: maruo@em.ist.hokudai.ac.jp).

Digital Object Identifier (inserted by IEEE).

Fig. 2. The mechanical contact depends on the particle density, insulation thickness and spring constant between particles. It is remarked that the resultant filling rate seldom changes when the number of particles is increased to 160.

III. Computation of Macroscopic Permeability

A. *Energy-based Evaluation*

The macroscopic complex permeability is evaluated by FEM based on the $A - \phi$ formulation, in which

$$\mathrm{rot}(\nu\,\mathrm{rot}\boldsymbol{A}) + j\omega(\boldsymbol{A} + \mathrm{grad}\phi) = \boldsymbol{0} \tag{4}$$

$$\mathrm{div}\{j\omega\sigma(\boldsymbol{A} + \mathrm{grad}\phi)\} = 0 \tag{5}$$

are solved, where ν, ω and σ denote the reciprocal of magnetic permeability, angular frequency and electric conductivity. The boundary conditions are shown in Fig.3. The power in the two-dimensional SMC domain Ω given by

$$\dot{P} = \frac{1}{2}\int_{\Omega} \sigma|\boldsymbol{E}|^2\, d\Omega + \frac{j\omega}{2}\int_{\Omega} \frac{|\boldsymbol{B}|^2}{\mu}\, d\Omega \tag{6}$$

is computed from the FE solution of (4) and (5). Introducing the macroscopic complex permeability $\langle\dot{\mu}\rangle$ of SMC that is constant over Ω, the power can also be written as

$$\dot{P} = \frac{j\omega}{2\langle\dot{\mu}\rangle^{*}}\int_{\Omega} |\boldsymbol{B}_0|^2\, d\Omega \tag{7}$$

where $*$ denotes complex conjugate. From (6) and (7), we have

$$\langle\dot{\mu}\rangle = \frac{\int_{\Omega}|\boldsymbol{B}_0|^2\, d\Omega}{\int_{\Omega}\frac{|\boldsymbol{B}|^2}{\mu}\, d\Omega - \frac{1}{j\omega}\int_{\Omega}\sigma|\boldsymbol{E}|^2\, d\Omega} \tag{8}$$

Taking the static limit $\omega \to 0$ in (8), we have the macroscopic permeability for static fields [2]

$$\langle\dot{\mu}\rangle = \frac{\int_{\Omega}|\boldsymbol{B}_0|^2\, d\Omega}{\int_{\Omega}\frac{|\boldsymbol{B}|^2}{\mu}\, d\Omega} \tag{9}$$

Note here that the second term in the denominator in (8) vanishes at the static limit because $\boldsymbol{E} = -j\omega(\boldsymbol{A} + \mathrm{grad}\phi)$.

B. *Consideration of Insulating Layer*

Figure 1 shows the generated SMC model which has the small overlaps among the particles, which are attributed to the numerical errors in DEM. The real SMC particles have a thin insulating layer on the surface of the particle. Since the insulating layer would be partially broken due to heating and pressure molding processes, the SMC particles would have partial magnetic or electric contacts among the neighbors. This contact is naturally modeled by the overlap resulted from DEM. When increasing the thickness of the insulating layer, the contact effects decrease.

To introduce the insulating layer into the SMC models generated by DEM, the permeability and electric conductivity in the surface layer of the SMC particle are changed to μ_0 and zero, respectively. By changing the thickness of the insulating layer, the contact effect as well as filling rate can be controlled.

C. *Ollendorff Formula*

The Ollendorff formula

$$\langle\mu_r\rangle = 1 + \frac{\eta(\mu_r - 1)}{1 + N(1-\eta)(\mu_r - 1)} \tag{10}$$

has been used to evaluate the macroscopic magnetic permeability $\mu_0\langle\mu_r\rangle$ of SMC [3, 4], where η and N are the filling rate and demagnetization factor, respectively. It has been shown that (10) is equivalent to Clausius-Mossotti formula as well as the Maxwell Garnet equation [7]. For consideration of the eddy currents induced in the iron particles in SMC, macroscopic complex permeability is obtained by substituting the complex permeability of a magnetic cylinder $\dot{\mu}_r$ [7]

$$\dot{\mu}_r = \mu_r \frac{J_1(z)}{zJ_0(z) - J_1(z)}, \qquad z = \sqrt{-j\omega\mu\sigma} \tag{11}$$

to (10), where J_n denotes the Bessel function of the n-th order. Note that we consider here the magnetic cylinder for comparison with the analysis mentioned in III.A, while the complex permeability of a magnetic sphere is given in [1]. Equations (10), (11) give the results that are consistent with those for the cell method with square cells.

TABLE I
Values of Physical Parameters in DEM

Number of particles	80
Density (particle) [kg/μm³]	0.5
Density (wall) [kg/μm³]	1×10⁴
Spring constant in normal direction (particle-particle) [N/μm]	1×10⁵
Spring constant in normal direction (particle-wall) [N/μm]	5×10⁵
Spring constant in shearing direction (particle-particle) [N/μm]	5×10³
Spring constant in shearing direction (particle-wall) [N/μm]	1×10³
Viscosity coefficient [Ns/μm²]	100
Dynamic friction coefficient (particle-particle)	10
Dynamic friction coefficient (particle-wall)	1
Time [s]	1×10⁻³
Steps	1.6×10⁵

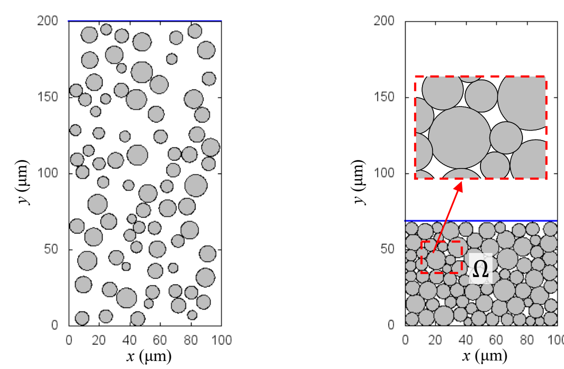

(a) Initial state (b) Final state
Fig. 1. Modeling result (First trial)

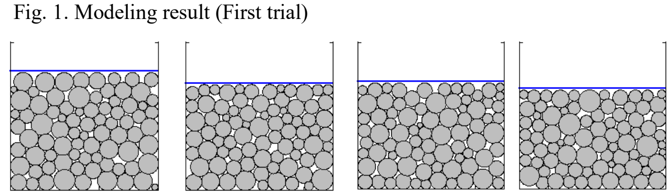

(a) Second trial (b) Third trial (c) Fourth trial (d) Fifth trial
Fig. 2. Modeling results starting from different states

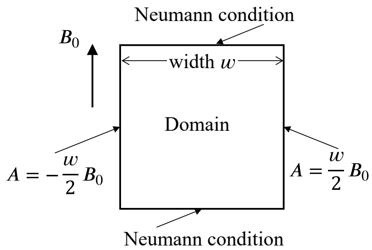

Fig. 3. Boundary condition

IV. Numerical Results

A. *Effect of Filling Rate*

We evaluate $\langle \dot{\mu} \rangle$ of SMC using the proposed method mentioned above. The SMC domain Ω is assumed to be immersed in a uniform magnetic field. The relative permeability of the iron particles is assume to be 100. The thickness of insulating layer of the particle is varied from 0.0μm to 0.6μm. Figure 4 shows the field distribution for different insulating layer thickness. The magnetic flux tends to go through the paths where the magnetic resistance is relatively small. The resultant macroscopic relative permeability of SMC models in Fig.1 (b) and Fig.2 is plotted against the filling rate that is controlled by the insulation thickness in Fig. 5. It is found that when the filling rate is low, the permeability computed by the present method is close to that computed by the Ollendorff formula that is valid for uniform particles without contact. The discrepancy between them increases with the filling factor. The present method gives the permeability which is close to the measured value [5] when the filling rate is about 0.85. This coincidence might not be important because the two-dimensional model with the assumed permeability of the iron particles is employed. What is important is that introduction of the magnetic contact, which occurs in a stochastic way among them, results in significant changes in the macroscopic permeability. The macroscopic permeability computed by the proposed method depends on the SMC model resulted from DEM. The deviation due to the differences in particle distribution is smaller than the discrepancy between the results obtained from the propose method and the Ollendorff formula.

B. *Effect of Inhomogeneity in Particle Size*

To study the effect of inhomogeneity in the SMC particle on the macroscopic permeability, a SMC model composed of uniform particles is generated using DEM. The particle radius is set to 5μm. The magnetic field distributions for different thickness of the insulating layer are shown in Fig. 6. It is found that the fluxes are rather uniform in comparison with those in Fig.4 although there are small disturbances from the edge effect near the domain boundary. Figure 7 shows the comparison of the macroscopic permeability of the uniform and non-uniform SMC models. It can be seen from Fig. 7 that the non-uniform SMC model provides the larger permeability. This might be due to the fact that the average number of adjacent particles in the non-uniform model is larger than that in the uniform model.

C. *Frequency Dependence*

We evaluate the frequency dependence of $\langle \dot{\mu} \rangle$ of the SMC

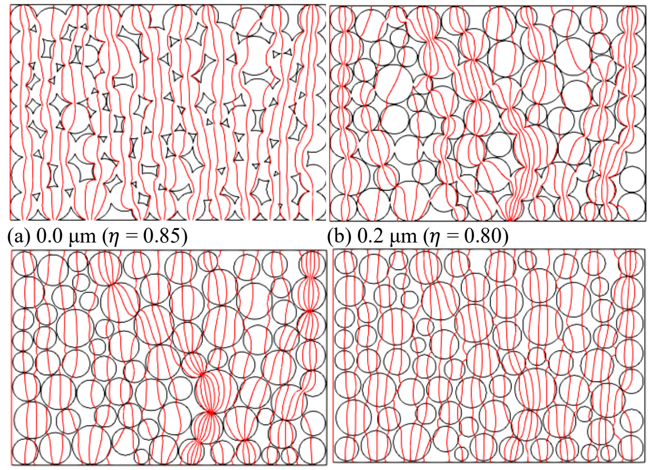

(a) 0.0 μm (η = 0.85) (b) 0.2 μm (η = 0.80)
(c) 0.4 μm (η = 0.73) (d) 0.6 μm (η = 0.67)

Fig. 4 . Flux lines for non-uniform particles with various insulation thickness

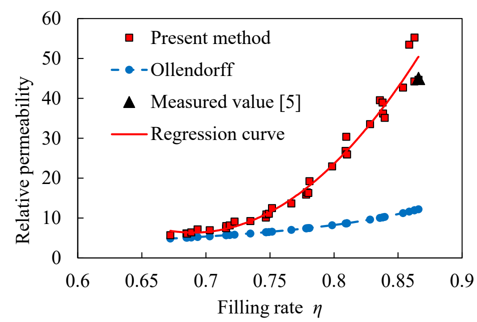

Fig. 5. Dependence of macroscopic permeability of SMC on filling rate

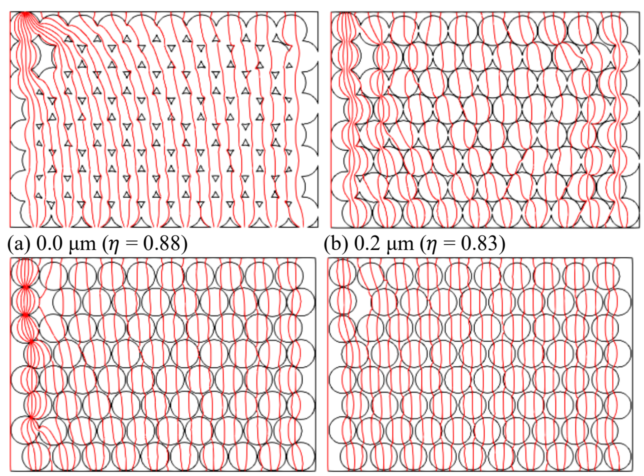

(a) 0.0 μm (η = 0.88) (b) 0.2 μm (η = 0.83)
(c) 0.4 μm (η = 0.76) (d) 0.6 μm (η = 0.70)

Fig. 6. Flux lines for uniform particles with various insulation thickness

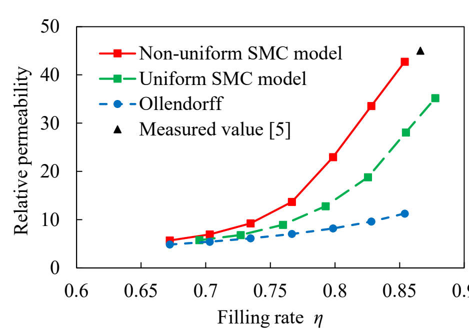

Fig. 7. Dependence of macroscopic permeability of SMC on filling rate

model in Fig. 1 using the proposed method. The SMC domain Ω is assumed to be immersed in an alternating magnetic field of angular frequency ω. The conductivity σ is set to 10^7 [S/m]. The frequency characteristic of $\langle\dot{\mu}\rangle$, computed from (8), is shown in Fig. 8, where the horizontal axis is the particle radius normalized by the skin depth. As frequency becomes higher, the real part of $\langle\dot{\mu}\rangle$ becomes smaller due to the response field effect of eddy currents. On the other hand, its imaginary part, which represents the eddy current loss, has peaks at different frequencies depending on the insulating thickness. Figure 9 shows magnetic fields for different frequencies when insulating thickness is 0.2 μm. We can see in Fig. 9 that the flux concentrates near the particle surface due to the skin effect when $a/\delta \geq 1$. The eddy current loss computed from

$$p_e = 2\omega \mathrm{Im}\left(\frac{B_0^2}{4\mu_0\langle\mu_r\rangle}\right) \tag{12}$$

is plotted for different insulating thickness in Fig. 10. The increase in the eddy current loss is not significant when the insulating thickness is greater than 0.4 μm.

D. *Anomaly Factor for Ollendorff Formula*

We modify Ollendorff formula (10) to consider the contact among particles which increases the permeability. The filling rate η in (10) is here modified to $\alpha\eta$, where α is an anomaly factor which is determined so that $\langle\dot{\mu}\rangle$ computed from (10) coincides with that computed by the proposed method at $\omega = 0$. Then, we calculate $\langle\dot{\mu}\rangle$ at different frequencies from (10) including the anomaly factor α. The SMC model in Fig. 1 with film thickness of 0.0 μm is analyzed, where the original filling rate is 0.85. The frequency dependence obtained from the modified Ollendorff formula, where $\alpha = 1.14$, and the proposed method are plotted in Fig. 11. It can be seen that this simple method provides a good approximation. This is found to be valid for other insulating thickness.

V. Conclusion

In this study, SMC is modeled using DEM considering inhomogeneity in particle size and magnetic and electric contact. The macroscopic permeability of SMC is evaluated through the energy-based formulation. It is found that the inhomogeneity in the particle size and possible contact among the particles can significantly increase the macroscopic permeability. Moreover, the Ollendorff formula modified with the anomaly factor gives a good approximation for the frequency characteristics. In future, we plan to extend the proposed method to the three-dimensional models. Moreover, magnetic saturation in SMC [8-9] will be considered.

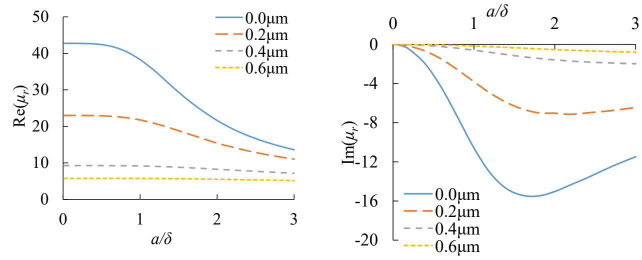

(a) Real part (b) Imaginary part

Fig. 8. Frequency characteristic of macroscopic complex permeability for different insulating thickness

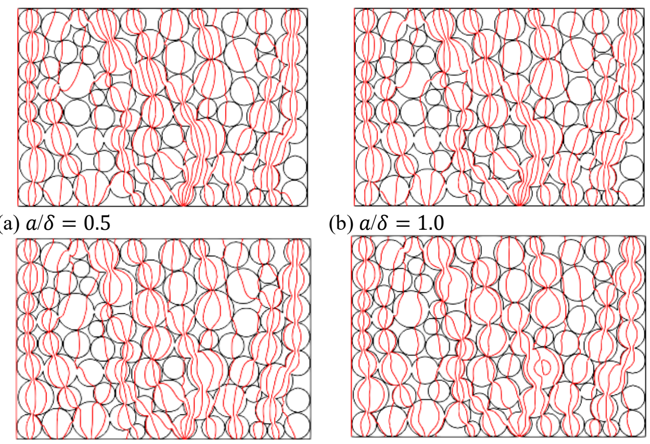

(a) $a/\delta = 0.5$ (b) $a/\delta = 1.0$

(c) $a/\delta = 1.5$ (d) $a/\delta = 2.0$

Fig. 9. Magnetic fluxes for different frequencies

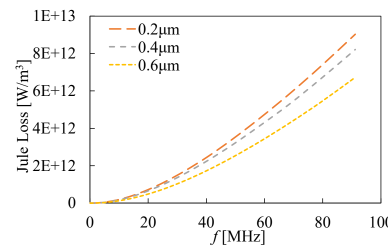

Fig. 10. Joule loss for different insulating thickness

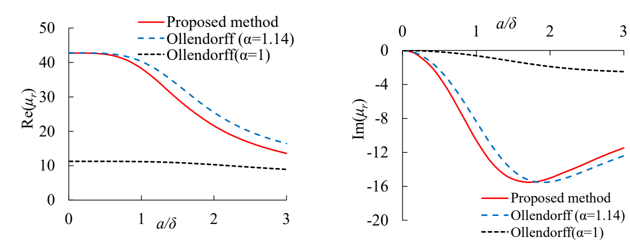

(a) Real part (b) Imaginary part

Fig. 11. Accuracy of modified Ollendorff formula considering contact

References

[1] A. Berthault, *et al.*, "Magnetic properties of permalloy microparticles," J. Magnetism and Magnetic Materials, vol. 112, pp. 477-480, 1992.

[2] H. Waki, *et al.*, "Estimation of effective permeability of magnetic composite materials," *IEEE Trans. Magn.*, vol. 41, no. 5, pp.1520-1523, 2005.

[3] F. Ollendorff, "Magnetostatik der massekerne," *Arch. f. Eledtrotechnik.*, 25, 1931, pp. 436-447

[4] T. Sato, *et al.*, "Loss computation of soft magnetic composite inductors based on interpolated scalar magnetic property," *IEEE Trans. Magn.*, vol. 51, no. 3, pp. 1-4, 2015, Art no. 8001704.

[5] Y. Ito, *et al.*, "Effect of magnetic contact on macroscopic permeability of soft magnetic composite," *IEEE Trans. Magn.*, vol. 52, no. 3, pp. 1-4, 2016, Art no. 9400804.

[6] P. A. Cundall and O. D. L. Strack, "A discrete numerical model for granular assemblies," *Geotechnique*, vol. 29, no. 1, pp. 47-65, 1979.

[7] H. Igarashi, "Semi-analytical approach for finite-element analysis of multi-turn coil considering skin and proximity effects," *IEEE Trans. Magn.,* vol. 53, no. 1, pp. 1-7, 2017, Art no. 7400107.

[8] H. Waki *et al.*, "Analysis of magnetic shielding effect of layered shields based on homogenization," *IEEE Trans. Magn*., vol.42, no.4, pp.847-850, 2006.

[9] T. Henneron *et al.*, "Nonlinear proper generalized decomposition method applied to the magnetic simulation of a SMC microstructure," *IEEE Trans. Magn*., vol.48, no.11, pp.3432-3245, 2012.